Proceedings Paper:

Perelli, A, Harput, S, De Marchi, L et al. (1 more author) (2013) Frequency warping compressive sensing for structural monitoring of aircraft wing. In: 2013 18th International Conference on Digital Signal Processing, DSP 2013. 18th International Conference on Digital Signal Processing, 01-03 Jul 2013, Fira, Santorini, Greece. IEEE . ISBN 9781467358057

https://doi.org/10.1109/ICDSP.2013.6622668

Frequency Warping Compressive Sensing for Structural Monitoring of Aircraft Wing

Alessandro Perelli*†, Sevan Harput†, Luca De Marchi* and Steven Freear†
*Department of Electrical and Information Engineering, University of Bologna, Italy
†Ultrasound Group, School of Electronic and Electrical Engineering, University of Leeds, United Kingdom
Email: alessandro.perelli2@unibo.it, s.harput@leeds.ac.uk, l.demarchi@unibo.it, s.freear@leeds.ac.uk

***Abstract*—This work focuses on an ultrasonic guided wave structural health monitoring (SHM) system development for aircraft wing inspection. The performed work simulate small, low-cost and light-weight piezoelectric discs bonded to various parts of the aircraft wing, in a form of relatively sparse arrays, for cracks and corrosion monitoring. The piezoelectric discs take turns generating and receiving ultrasonic guided waves. The development of an in situ health monitoring system that can inspect large areas and communicate remotely to the inspector is highly computational demanding due to both the huge number of Piezoelectric sensors needed and the high sampling frequency. To address this problem, a general approach for low rate sampling is developed. Compressive Sensing (CS) has emerged as a potentially viable technique for the efficient acquisition that exploits the sparse representation of dispersive ultrasonic guided waves in the frequency warped basis. The framework is applied to lower the sampling frequency and to enhance defect localization performances of Lamb wave inspection systems. The approach is based on the inverse Warped Frequency Transform (WFT) as the sparsifying basis for the Compressive Sensing acquisition and to compensate the dispersive behaviour of Lamb waves. As a result, an automatic detection procedure to locate defect-induced reflections was demonstrated and successfully tested on simulated Lamb waves propagating in an aluminum wing specimen using PZFlex software. The proposed method is suitable for defect detection and can be easily implemented for real application to structural health monitoring.**

***Keywords*—Lamb waves, Warped frequency transform, Compressive sensing, Defect detection, Aircraft wing.**

I. Introduction

Damages to aircraft and high-speed vehicles caused by the impact of debris and flying objects is a critical concern for automotive and aeronautic systems. Such damages, in fact, if not detected and repaired at an early stage might grow leading to the failure of the systems. Traditionally, visual inspection, accompanied by ultrasound bulk wave or eddy current technology, is often used to obtain general information on the structural health conditions. However, the inspection is limited to a point-by-point manner and is very time consuming. In most cases, erection of scaffolding or disassembly of the structure is needed to inspect the interior and inaccessible components, being very labour intensive and possibly resulting in maintenance-induced damages. In this context, Structural health monitoring (SHM) technologies can allow for an automatic detection of defects due to impacts. Among the number of SHM approaches, the one based on guided waves (GW) is considered as the most promising and versatile. Some major advantages of this technique include fast scanning capabilities, low cost, long-range inspection, and testing inaccessible or complex components.

Recently, small and conformal piezoelectric ceramics and wafer transducers, either being surface mounted or embedded leave-in-place on the structures, have been widely studied for generating and receiving guided waves for structural integrity monitoring. In fact, an impact at high speed produces detectable acoustic and ultrasonic guided waves on the structural component. These waves can be used to compute the location of the impact and eventually to assess the damage. In general, GW based technologies for SHM exploit a network of piezoelectric transducers positioned on the structure to inspect. The minimization of the number of array elements is fundamental to reduce not only the hardware complexity associated with transducer wiring and multiplexing circuitry but also the intensive signal processing of the large amounts of recorded data. For this reason, there is growing interest in minimizing the number of sensors by optimizing their positioning, as well as by increasing the resolution of impact localization procedures [1].

Another current trend in the SHM field is to create wireless sensor networks with low power consumption or even energetically autonomous [2], [3]. One promising solution would be a SHM system that could be embedded into the structure, inspect the structural hot spots and download data or diagnostic results wirelessly to a remote station [4], [5], [6].

A lot of literature has been produced on the use of sensor-array-based methods for high-speed acquisition and data processing. However, generally such approaches use a large number of individual sensors that usually are bulky, heavy and require wiring back to a central location. Moreover when large-scale deployment are implied, the power consumption of the system is hardly sustainable by the ordinary generation system present on board. Recent works in the area of time-frequency representations (TFRs) [7] [8] show great promise for applications in nondestructive evaluation and material characterization, in particular to interpret ultrasonic GWs, as they represent a class of complicated ultrasonic signals, exhibiting dispersion and containing multiple modes. Nevertheless, the identification of Lamb modes is a challenging step in the process of damage detection.

This work proposes a time-frequency (TF) energy density function approach that makes use of known dispersion characteristics for a propagating wave mode in order to locate defects in aircraft wing structures.

Compressive Sensing (CS) [9] is an alternate framework to the traditional Shannon-Nyquist framework of digital signal and image acquisition. CS can be viewed as a scheme for simultaneous sensing and compression; instead of being proportional to the Fourier bandwidth, the rate of data acquisition need only be proportional to the sparsity of the signal, the number of nonzero coefficients of a signal representation in some basis. Many methods for signal compression are commonly based on the transform coding approach. In such methods, the assumption is that a signal $x \in \mathbb{R}^N$ can be represented as a sparse linear combination of elements from a fixed, known basis $\Psi \in \mathbb{R}^{N \times N}$. This has given rise to the design and development of sophisticated compression algorithms that operate on a given signal x according to structured sparsity models [10], [11].

In this work the compressive acquisition of Lamb wave signal for damage detection is studied; this new framework is based on the Warped Frequency Transform to achieve a sparse representation of the signal. In particular an acquisition and reconstruction stage is developed to obtain the sparse reflection due to the damage in the warped domain.

The rest of the paper is organized as follows: Section II provides a brief review of the Warped Frequency Transform; in Section III we provide an overview of the Compressive Sensing Framework and the proposed framework to recover the reflectivity function due to the damage in the warped domain. Finally in Section V we show the validation of the proposed framework and the effectiveness of the obtained results.

II. Frequency Warping Signal Processing

A. Frequency Warping Transform

The first step is related to the design of a proper basis for the Lamb waves in order to obtain a sparse representation; such sparsifying dictionary can be obtained by using unitary transformations. Lamb waves are mechanical-stress waves which propagate along solid surface of finite dimension. In a given waveguide (e.g., a plate, rod, or rail) one or more GWs can exist at a given frequency. In general, each GW has a frequency-dependent propagation speed so a dispersive behaviour. The representation of the wave velocity versus frequency is generally referred to as its dispersion curve. Dispersion generates nonstationary signals when the waveguide is excited by a broadband pulse.

The unitary operators based on frequency warping can be used for the analysis of GWs. These operators deform the frequency axis with a warping function $w(f)$ [12]. To guarantee invertibility of this process, $w(f)$ must be chosen so that

$$\frac{dw(f)}{df} \doteq \dot{w}(f) > 0 \quad \Rightarrow \exists w^{-1},\, w^{-1}(w(f)) = f$$

where $\dot{w}$ represents the first derivative of the map w with respect to frequency and w^{-1} is the functional inverse of w. Given a generic signal $s(t)$ whose continuous Fourier transform is $\mathbb{F}s(t) \doteq S(f)$, the continuous warping operator $\mathbf{W}$ is defined as

$$(\mathbb{F}\mathbf{W}s)(f) = \sqrt{\dot{w}(f)}(\mathbb{F}s) \cdot (w(f))$$

The warping operator results in a unitary transformation which preserves orthogonality [13]. For discrete-time signals of finite duration N, the warping operator is defined as a matrix whose entries are

$$\mathcal{W}(m,n) = \frac{1}{M}\sum_{k=0}^{M-1} \sqrt{\dot{w}\left(\frac{k}{M}\right)} e^{j2\pi(m\frac{k}{M} - nw(\frac{k}{M}))}, \quad m \in \mathbb{Z}_M, \quad n \in \mathbb{Z}_N$$

By considering the discrete Fourier transform of size $M \times M$,

$$\mathcal{F}(k,n) = e^{-j2\pi n \frac{k}{M}}, \quad k,n \in \mathbb{Z}_M$$

and the nonuniform discrete Fourier transform of size $M \times N$, scaled along rows according to the orthogonalizing factor $\sqrt{\dot{w}\left(\frac{k}{M}\right)}$

$$\mathcal{F}_w(k,n) = \sqrt{\dot{w}\left(\frac{k}{M}\right)} e^{-j2\pi n w(\frac{k}{M})}, \quad k \in \mathbb{Z}_M,\ n \in \mathbb{Z}_N \tag{1}$$

the discrete warping operator in (1) can be factorized as

$$\mathcal{W}(m,n) = \mathcal{F}^{-1}\mathcal{F}_w$$

A fast computation of the discrete warping operator is achieved by means of this decomposition. In fact, $\mathcal{F}^{-1}$ is computed with the Fast Fourier transform (FFT) and $\mathcal{F}_w$ can be efficiently factorized with the nonuniform-FFT algorithm [14]. In order to compensate the signal with respect to a particular guided mode, $w(f)$ can be defined through its functional inverse, as:

$$C\frac{dw^{-1}(f)}{df} = \frac{1}{c_g(f)} \tag{2}$$

where $\frac{1}{c_g(f)}$ is the nominal dispersive slowness relation of the wave we want to consider, being $c_g(f)$ its group velocity curve and C is a normalization parameter selected so that $w^{-1}(0.5) = w(0.5) = 0.5$. Equivalently, the inverse warping map w^{-1} can be defined with respect to the wave phase velocity $c_{ph}(f)$ or wavenumber $k(f)$.

The group velocity curves of the Lamb modes for a 0.003 m thick aluminium wing as in Figure 4 with Young modulus $E = 69$ GPa, Poisson's coefficient $\nu = 0.33$ and material density $\rho = 2700$ kg $\cdot$ m^{-3} are represented in Fig. 1. The curves were obtained by using PZFlez software. A sample warping map is depicted in Fig. 2 along with its functional inverse.

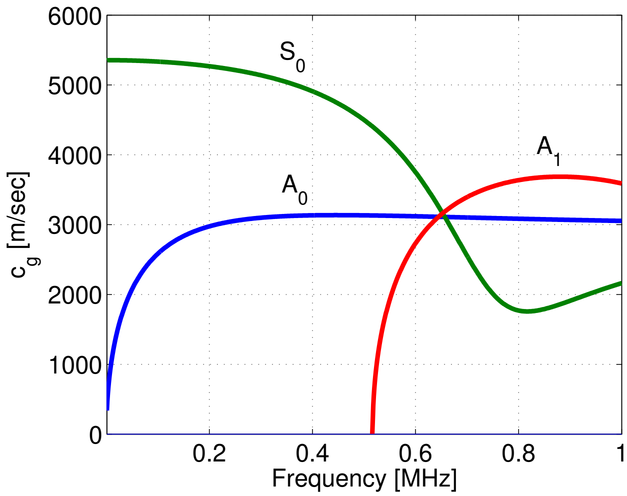

Fig. 1. $c_g(f)$ dispersion curves for the Lamb waves propagating in an aluminium 0.003 m aluminum wing obtained by simulation.

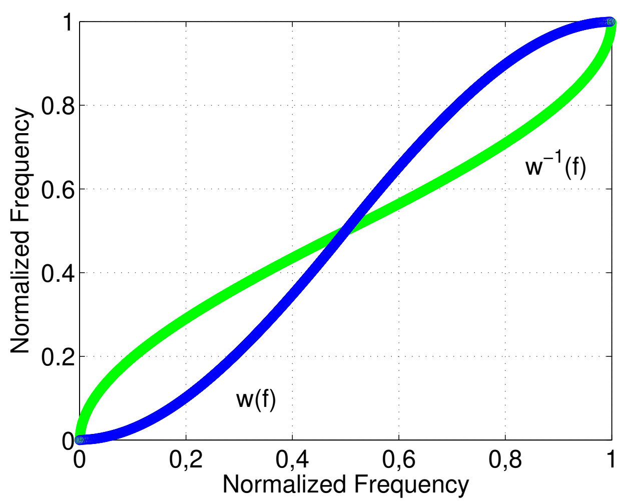

Fig. 2. Warping map $w(f)$ for A_0 wave dispersion compensation and its functional inverse $w^{-1}(f)$ designed according to Eq. 2.

B. Dispersion Compensation

In active monitoring techniques the time instant in which an acoustic emission starts is known. Being $(\mathbb{F}s_0)(f,0)$ the Fourier Transform of the excited wave (incipient pulse centered in $t = 0$), an undamped guided wave at a distance D from the source point, $s(t,D)$, can be modeled in the frequency domain as a dispersive system whose response is:

$$(\mathbb{F}s)(f,D) = (\mathbb{F}s_0)(f,0) \cdot e^{-j2\pi \int \tau(f,D)df} \tag{3}$$

being $\tau(f,D)$ the group delay of the wave component of frequency f which can be assumed equal to:

$$\tau(f,D) = \frac{D}{c_g(f)} = D \cdot C \cdot \frac{dw^{-1}(f)}{df} \tag{4}$$

By substituting Eq. 4 into Eg. 3:

$$(\mathbb{F}s)(f,D) = (\mathbb{F}s_0)(f,0) \cdot e^{-j2\pi w^{-1}(f)CD} \tag{5}$$

where the distortion results from the nonlinear phase term. Consider now that the generated dispersive wave $s(t)$ is acquired after having travelled the distance of propagation, D_1. The warped Fourier transforms of the recorded signals $s(t,D_1)$ is given by:

$$(\mathbb{F}\mathbf{W}s(t,D_1))(f) = \sqrt{\dot{w}(f)} \cdot (\mathbb{F}s_0)(w(f),0) \cdot \underline{e^{-j2\pi f C D_1}} \tag{6}$$

where the right hand terms can be distinguished only for the underlined distance-dependent linear phase shifts, which causes simple translations of the warped signals on the warped time axis.

III. Frequency Warping Compressed Sensing

A. General Framework

The main idea behind CS is now quite well known but, for the sake of completeness, the main concepts are summarized. Let $x = \Psi\alpha$ be a real-valued N-dimensional discrete signal vector ($x \in \mathbb{R}^N$) that is compressible in some orthonormal basis $\Psi = [\psi_1|\psi_2|\ldots|\psi_N]$, where each column is a vector ψ_i, and α represents the N-dimensional coefficient vector. In our framework the orthonormal basis Ψ is represented by the discrete warping operator $\mathcal{W}(m,n)$ defined in Section II. By compressible we mean that the entries of $\alpha = [\alpha_1, \alpha_2, \ldots, \alpha_N]$, when sorted in decreasing order of magnitude, decay rapidly to zero; any such a signal is well approximated using a K-term approximation, consisting of the K largest entries of α and setting all other terms to zero

$$x \approx \sum_{k=1}^{K} \alpha_k \psi_k, \quad \text{with} \quad K \ll N.$$

In essence, compressible signals are well approximated by sparse signals. Conventionally, one would collect signal samples at the Nyquist rate forming x and then compress it using nonlinear digital compression techniques. CS offers a striking alternative by showing that if x is compressible, one can recover to a K-term approximation by only collecting roughly $M \approx K$ samples using simple analog measurement waveforms, thus sensing and compressing at the same time. More precisely, $M = O(K \log N/K)$ samples are collected by projecting on sensing waveforms $\{\phi_i\}_{1 \le i \le M}$ thus forming the measurement vector $y_i = \phi_i^H x = \langle \phi_i, x \rangle$, $i = 1, \ldots, M$. Consequently, the CS linearly compressed data vector $y \in \mathbb{R}^M$ is described by $\mathbf{y} = \mathbf{\Phi x}$, where $\mathbf{\Phi}$ denotes the $M \times N$ measurement or sensing matrix with the vectors $\phi_1^H, \ldots, \phi_M^H$ as rows. It is important to notice that the sensing matrix $\mathbf{\Phi}$ does not depend on the signal: CS proposes a simple linear sampling strategy that is only marginally off the optimal but complex best adaptive strategy. To guarantee the robust and efficient recovery of any S-sparse signal, the sensing matrix $\mathbf{\Phi}$ must obey the key restricted isometry property (RIP)

$$(1 - \delta_S)\|\alpha\|_2^2 \le \|\mathbf{\Phi\Psi}\alpha\|_2^2 \le (1 + \delta_S)\|\alpha\|_2^2$$

for all S-sparse vectors α. The isometry constant δ_S of matrix $\mathbf{\Phi}$ must not be too close to one. This property is difficult to verify in practice and it is often replaced by the requirement that the sensing matrix $\mathbf{\Phi}$ and sparsity basis $\mathbf{\Psi}$ must be incoherent, i.e., their coherence

$$\mu(\mathbf{\Phi}, \mathbf{\Psi}) = \sqrt{N} \cdot \max_{1 \le k,j \le N} |\langle \phi_k, \psi_j \rangle|$$

is small enough. A universal good choice for the sensing matrix $\mathbf{\Phi}$ are random matrixes, such as random matrixes with independent identically distributed entries formed by sampling: 1) a Gaussian distribution; 2) a symmetric Bernoulli distribution. If the RIP holds, then accurate reconstruction can be accomplished by solving the following convex optimization problem:

$$\min_{\widetilde{\alpha} \in \mathbb{R}^N} \|\widetilde{\alpha}\|_1 \quad \text{subject by} \quad \|\mathbf{\Phi}\mathbf{\Psi}\widetilde{\alpha} - \mathbf{y}\|_2 \le \sigma$$

where σ bounds the amount of noise unavoidably corrupting the data. Many algorithms were introduced to solve this l_1-norm reconstruction problem; our results are based on the orthogonal matching pursuit algorithm [15].

IV. Analog Compressive Sampling Acquisition

Suppose our analog signal has finite information rate K i.e., the signal can be represented using K parameters per unit time in some continuous basis. More concretely, let the analog signal $x(t)$ be composed of a discrete, finite number of weighted continuous basis or dictionary components

$$x[i] = \sum_{n=1}^{N} \alpha_n \psi_n[i] \tag{7}$$

with $t, \alpha_n \in \mathbb{R}$. In cases where there are a small number of nonzero entries in α, we may again say that the signal x is sparse. Although each of the dictionary elements ψ_n may have high bandwidth, the signal itself has few degrees of freedom. Our signal acquisition system consists of three main components; demodulation, filtering, and uniform sampling. As seen in Figure 3, the signal is modulated by a psuedo-random maximal-length PN sequence of ± 1. This chipping sequence $p_c(t)$ must alternate between values at or faster than the Nyquist frequency of the input signal. The purpose of the demodulation is to spread the frequency content of the signal so that it is not destroyed by the second stage of the system, a low-pass filter with impulse response $h(t)$. Finally, the signal is sampled at rate M using a traditional ADC. Although our system involves the sampling of continuous-time signals, the discrete measurement vector y can be characterized as a linear transformation of the discrete coefficient vector α. As in the discrete CS framework, we can express this transformation as an $M \times N$ matrix $\mathbf{\Theta} = \mathbf{\Phi}\mathbf{\Psi}$ that combines two operators: $\mathbf{\Psi}$, which maps the discrete coefficient vector α to an analog signal x, and $\mathbf{\Phi}$, which maps the analog signal x to the discrete set of measurements y. To find the matrix $\mathbf{\Theta}$ we start by looking at the output $y[m]$, which is a result of convolution and demodulation followed by sampling at rate M. Since our analog input signal in Eq. 7 is composed of a finite and discrete number of components of $\mathbf{\Psi}$, we can write

$$y[m] = \sum_{n=1}^{N} \alpha_n \int_{-\infty}^{+\infty} \psi_n(\tau) p_c(\tau) h(mM - \tau) d\tau$$

It is now clear that an expression for each element $\theta_{m,n} \in \mathbf{\Theta}$ can be separated out for row m and column n

$$\theta_{m,n} \int_{-\infty}^{+\infty} \psi_n(\tau) p_c(\tau) h(mM - \tau) d\tau$$

The CS acquisition scheme is shown in Figure 3

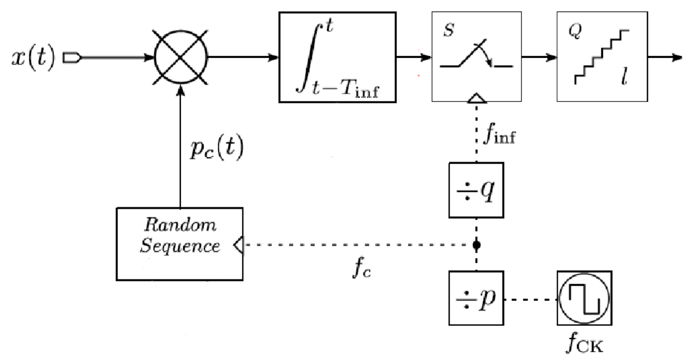

Fig. 3. Compressed Sensing acquisition scheme: random modulation pre-integration

V. Verification

A. Simulations

Finite element analysis of an aircraft wing was performed by PZFlex (Weidlinger Assoc. Inc. CA) and, as a case study, the proposed framework was exploited to locate defects in an aluminum 1050A wing 1000 $\times$ 1000 mm and 3 mm thick. Four piezoelectric discs (PIC181, diameter 10 mm, thickness 1 mm) were bonded to the wing. The simulated setup designed with Solidworks (Dassault Systmes ,USA)is shown in Fig. 4 and the position of the transducers is defined in Table I.

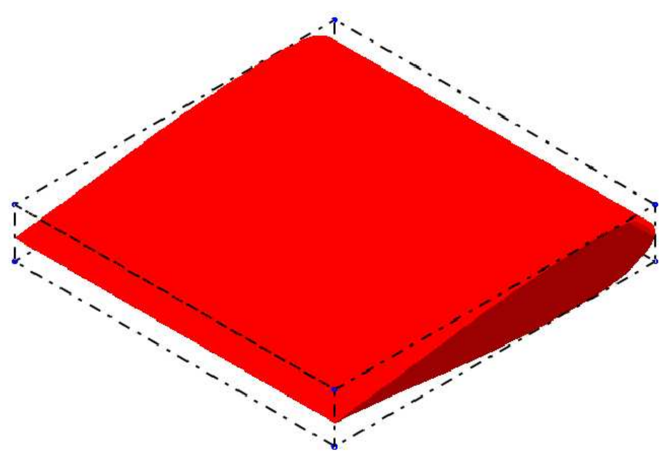

Fig. 4. Simplified aircraft wing model used in the simulations. Simulated set up used to validate the defect location procedure with PZFlex and Solidworks CAD importing

TABLE I
ACTUATOR AND RECEIVERS TOPOLOGY.

Coordinates	Actuator	Receivers		
x (m)	0.10	0.10	0.90	0.90
y (m)	0.10	0.70	0.10	0.70

The sampling frequency chose for the simulations was $f_s = 500$ kHz, sufficiently high to avoid aliasing effects, as the frequency content of the acquired signals vanishes above 60 kHz. The active monitoring was performed by simulating a chirp as voltage input in $(0.1, 0.1)$ m on the top of the surface (active piezoelectric discs) and recording the wave propagation by two sensors on the top surface. In PZFlex simulation the structural damage was emulated as a cubic mass of 10 mm on the top of the wing surface [16]. For example, the waveforms detected by the 3 receivers, after having placed the mass at the coordinates $x = 0.20$ m and $y = 0.55$ m, are shown in Fig. 5.

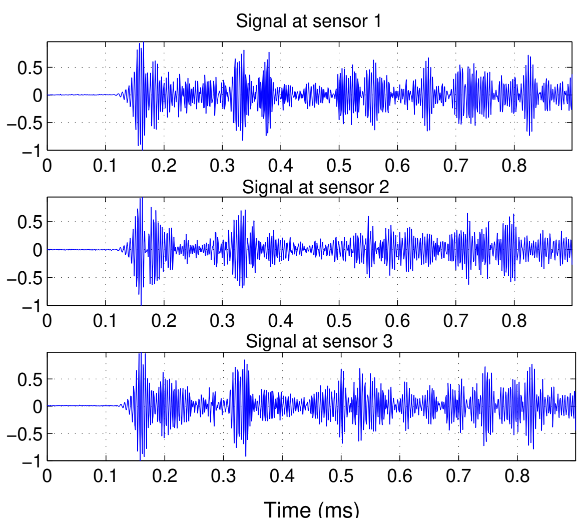

Fig. 5. Simulated signals acquired by the 3 sensors whose coordinates are reported in Table I.

As can be seen from the time waveforms, it is difficult estimating the time of arrival of echoes due to the mass (emulated defect) among the other interfering waves caused by edge reflections and multimodal propagation.

The acquired signals were processed through the random modulator pre-integrator implemented in Matlab (Mathworks Inc., MA) with the frequency specifications are the following: chipping frequency equal to 500 kHz and the information frequency $f_{inf} = 50$ kHz.

In order to compensate for dispersion, first the WFT operator must be defined. In the $[0-300]$ kHz frequency range, only the two fundamental A_0 and S_0 Lamb waves can propagate through this plate. The group velocity curve of the A_0 mode was used to shape the warping operator according to Eq. 2 because the energy in the A_0 mode is considerably greater than that retained by the S_0 mode for out-of-plane excitation.

In the recovery stage the orthogonal matching pursuit algorithm was applied to recover the sparse signal in the warped domain. Fig. 6 shows the sparse estimated signal related to the defect located in $x = 0.20$ m and $y = 0.55$ m and the passive sensor 2 at 0.6 m from the active sensor. The local maxima of the reconstructed sparse signal are close to the real distance of the incident wave (blue) and the distance due to the reflection of the defect (green). The warped distance can be detected and the corresponding coordinates provide the distance traveled by the incident wave and the total distance of the wave reflected by the defect.

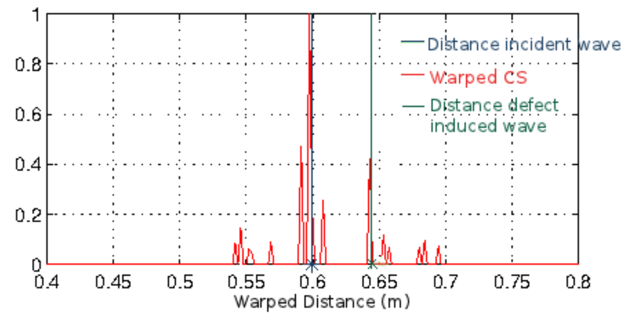

Fig. 6. Sparse signal after the CS recovery

B. Results

To asses the feasibility of the proposed technique, a study on the dependence of the localization error with the number of bit used in the quantization stage was performed. In Table II the localization error and the mean absolute error (%) which is defined as the between the localization error and the actual defect position are shown.

TABLE II
LOCALIZATION ERROR DEPENDENCY ON THE QUANTIZATION.

Number of Bits	Localization Error (mm)	Mean absolute error
8	19.3	2.9%
16	8.7	1.3%
24	3.1	0.5%

It is possible to see how using few bits, for example 8 bits, the error tends to rise reaching 2 cm. The choice of the number of bits depends on the specific control and application; a good compromise can be between 16-24 bits.

It is important to notice how the obtained results with the CS framework are very close to the localization error achieved applying only the compensation operator without lowering the sampling frequency using the random modulator as acquisition module.

In Fig. 7 the localization error comparison between compensation with and without Compressed Sensing acquisition is presented. It is possible to underline that the performance of the CS proposed algorithm was very close with the simple dispersion compensation warping procedure.

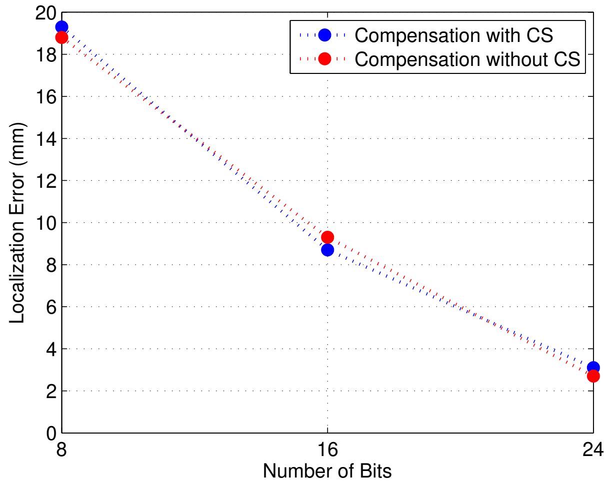

Fig. 7. Localization error comparison between compensation with and without Compressed Sensing acquisition

VI. Conclusion

In this work, a signal processing strategy to locate defects in aircraft wings by analysing actuated and received Lamb waves by piezoelectric sensors was proposed. The method is suitable for chirped pulse actuations, and it is based on a two-step procedure using the Compressed Sensing acquisition method. The signal processing reveals directly the distance traveled by the dispersive waves thus overcoming the difficulties associated to arrival time detection. In particular, by exploiting the dispersion compensation properties of the WFT a suitable sparse representation of Lamb wave is obtained. The actuated frequency modulated chirp is compressed in a subsequent processing step. A mean absolute error on defects localization equal to 0.5% is obtained simulating the dispersive propagation on a simplified aircraft wing through PZFlex. It is worth noticing that the robustness of the distance estimation allows to achieve such performances with sparse arrays of conventional transducers. Thanks to its unique potential, the WFT joint with CS acquisition could pave a new class of procedures to locate defects in waveguides. Optimization and adaptive selection of the array shape and size are under investigation to further improve the accuracy of the proposed approach.

References

[1] A. Perelli, L. D. Marchi, A. Marzani, and N. Speciale, "Acoustic emission localization in plates with dispersion and reverberations using sparse pzt sensors in passive mode," *Smart Mater. Struct.*, vol. 21, no. 2, p. 025010, 2012.

[2] D. Boyle, M. Magno, B. O'Flynna, D. Brunelli, E. Popovici, and L. Benini, "Towards persistent structural health monitoring through sustainable wireless sensor networks," in *Intelligent Sensors, Sensor Networks and Information Processing (ISSNIP), 2011 Seventh International Conference on*, 2011, pp. 323–328.

[3] L. Benini, D. Brunelli, C. Petrioli, and S. Silvestri, "Genesi: Green sensor networks for structural monitoring," in *Sensor Mesh and Ad Hoc Communications and Networks (SECON), 2010 7th Annual IEEE Communications Society Conference on*, 2010, pp. 1–3.

[4] X. Zhao, T. Qian, G. Mei, C. Kwan, R. Zane, C. Walsh, T. Paing, and Z. Popovic, "Active health monitoring of an aircraft wing with an embedded piezoelectric sensor/actuator network: Ii wireless approaches," *Smart Mater. Struct.*, vol. 16, pp. 1218–1225, 2007.

[5] L. Liu and F. Yuan, "Active damage localization for plate-like structures using wireless sensors and a distributed algorithm," *Smart Mater. Struct.*, vol. 17, p. 055022, 2008.

[6] B. Aygun and V. Gungor, "Wireless sensor networks for structure health monitoring: recent advances and future research directions," *Sensor Review*, vol. 31, no. 3, pp. 261–276, 2011.

[7] R. Benz, M. Niethammer, S.Hurlebaus, and L. J. Jacobs, "Localization of notches with lamb waves," *Journal of the Acoustical Society of America*, vol. 114, no. 2, pp. 677–685, 2003.

[8] A. Leger and M. C. Deshamps, *Ultrasonic Wave Propagation in Non Homogeneous Media*. Springer, 2009.

[9] D. Donoho, "Compressed sensing," *IEEE Transactions on Information Theory*, vol. 52, no. 4, pp. 1289–1306, 2006.

[10] R. Baraniuk, V. Cevher, M. Duarte, and C. Hegde, "Model-based compressive sensing," *IEEE Transactions on Information Theory*, vol. 56, no. 4, pp. 1982–2001, 2010.

[11] C. Hegde and R. Baraniuk, "Sampling and recovery of pulse streams," *IEEE Transactions on Signal Processing*, vol. 59, no. 4, pp. 1505–1517, 2011.

[12] A. Oppenheim and D. Johnson, "Discrete representation of signals," *Proceedings IEEE*, vol. 60, no. 6, pp. 681–691, 1972.

[13] L. D. Marchi, A. Marzani, S. Caporale, and N. Speciale, "Ultrasonic guided-waves characterization with warped frequency transforms," *IEEE Trans. Ultrason. Ferroelectr., Freq. Control*, vol. 56, pp. 2232–2240, 2009.

[14] J. Fessler and B. Sutton, "Nonuniform fast fourier transforms using min-max interpolation," *IEEE Trans. Signal Process*, vol. 51, no. 2, pp. 560–573, 2003.

[15] D. Needell and J. Tropp, "Cosamp: Iterative signal recovery from incomplete and inaccurate samples," *Applied and Computational Harmonic Analysis*, vol. 26, no. 3, pp. 301–321, 2009.

[16] L. D. Marchi, A. Perelli, and A. Marzani, "A signal processing approach to exploit chirp excitation in lamb wave defect detection and localization procedures," *Mechanical Systems and Signal Processing*, 2012.